

# A FPGA-Based Replacement for a Network Analyzer in an Instrumentation-Based 200 GHz Radar

By John Mower and Yasuo Kuga

Presenting a method for constructing a dedicated 200 GHz radar.

We are entering an exciting time where millimeter-wave (MMW) systems are encroaching into everyday life, examples being communications, auto-navigation, and security. It is instinctive to consider these systems in industrial settings, as well. Given the current energy climate, it may be possible to apply MMW technology in an effort to improve efficiency in power generation industries. Paper is one such industry, specifically in the Kraft-Recovery process. In the Kraft process, pulping salts and organic compounds, byproducts of extracting fiber from wood, are retrieved through combustion. The process of incinerating the solution generates a surplus of heat that is reclaimed in the form of process- and power generating- steam. Heavy sooting of salt in the heat-exchanger is normally experienced and a MMW imaging system was proposed to measure these deposits to aid in the reduction of maintenance steam consumption. Imaging at 200 GHz is attractive due to the electrical properties of the salts as well as the need for millimeter scale resolution; however, wide-band imaging systems operating at these frequencies are generally built from instrumentation and a need for dedicated hardware exists. To this end, we will present a method for constructing a dedicated 200 GHz radar and the requisite signal processing techniques for such an imaging system.

Our previous research developed a stepped-frequency continuous-wave (SFCW) 200 GHz, 20 GHz bandwidth, imaging radar capable of measuring soot thickness deposited on boiler tubes (Figure 1). This radar uses a NWA as a sweep source and receiver. A dedicated and lower-cost unit was desired, inspiring the construction of a FPGA-based demonstrator. A favorable comparison of both the NWA- and FPGA-based systems will be presented in this article.

## NWA-Based System

The NWA-based system utilizes a microwave transceiver and V05VNA2 - series OML 140-220 GHz frequency extension modules. Our work has shown that a system operating around 200 GHz with at least 20 GHz bandwidth is optimal for imaging the salt buildup in the boiler. Shown in Figure 2, the NWA acts as a RF sweep source and digital acquisition system for a 181 – 216 GHz radar. With several key points to design around, we set out to build a dedicated system that had at least 20 GHz bandwidth, high Signal to Noise Ratio (SNR), long-term phase-stability, and fast sweep-time. The dedicated FPGA-based system reuses much of the existing system while removing the NWA, the 61.041667 MHz LO, and the components used to create the 2nd IF in Figure 2. In the FPGA-based system, the 1st IF ( $a_{1st}$  and  $b_{1st}$ ) is under-sampled by a Hittite Microwave HMCAD1520 ADC (14 bit resolution) and real-time baseband conversion/filtering is processed on a SP601 Xilinx Spartan-6 FPGA board. Control and communication is facilitated by a processor core on the FPGA while the sweep-IF is created by a Linear Technologies 6946-3 PLL+VCO evaluation board (see Figure 3). The NWA is then essentially replaced by three development boards and a remote computer for post-processing (Figure 4).

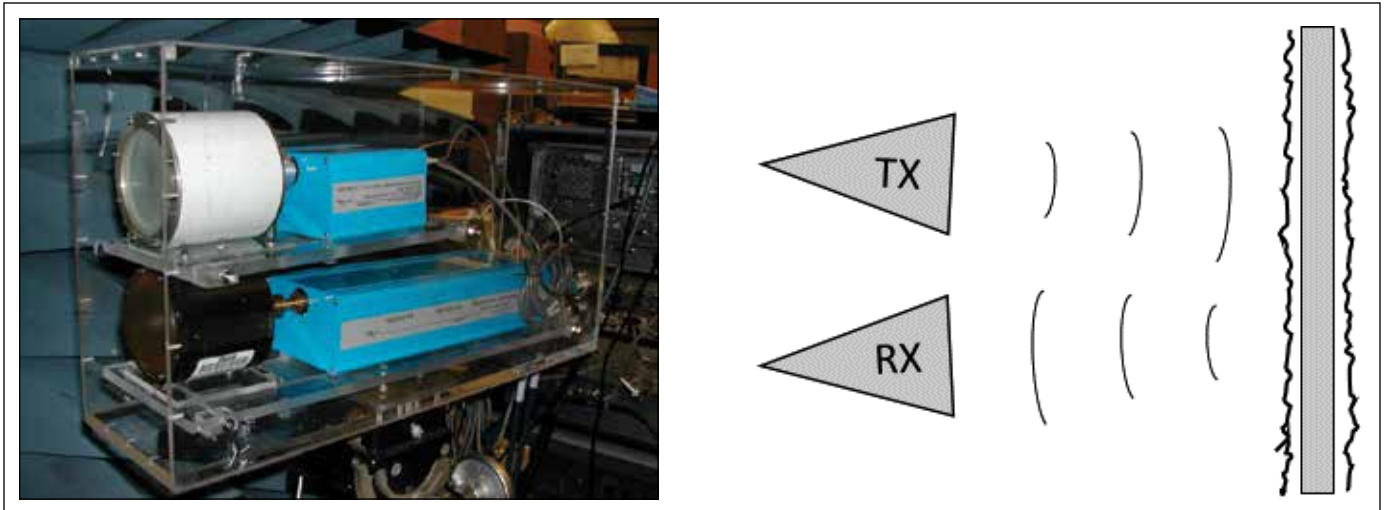


Figure 1 • Left, 200 GHz OML frequency extenders and lens-antennas in air-conditioned box (shielding removed) for experimental imaging of Kraft boilers. Right, radar images tubes and measured the salt buildup.

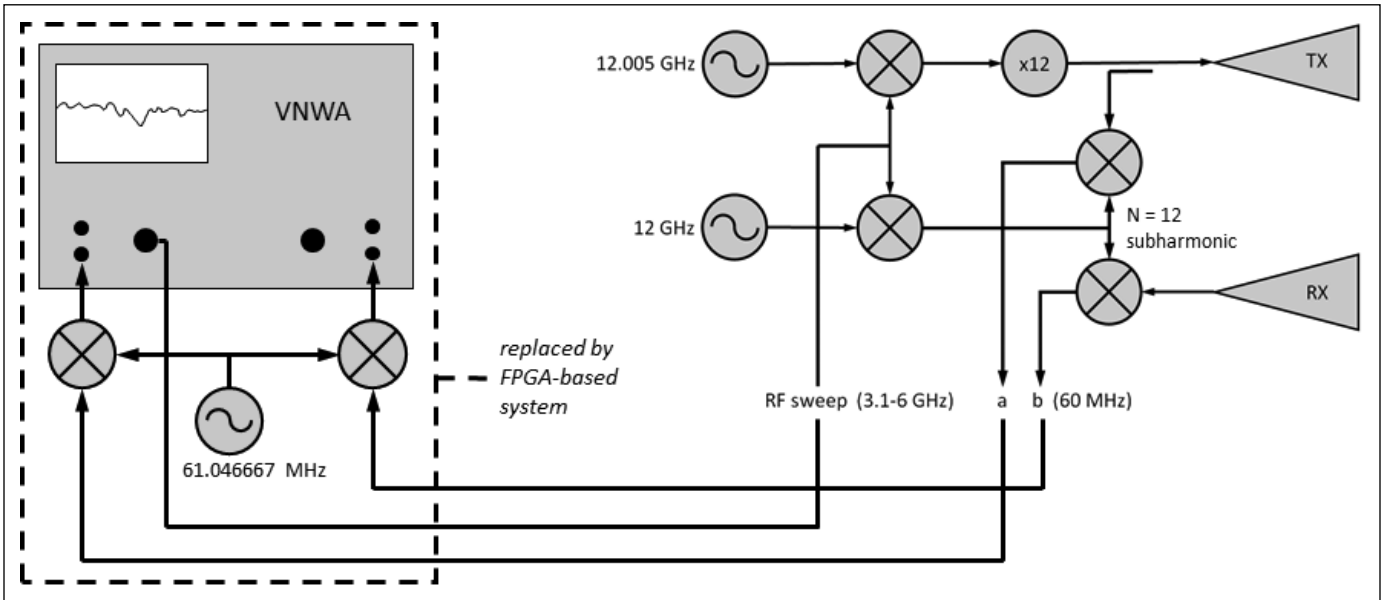


Figure 2 • Two sources at 12005 and 12000 MHz are mixed with the sweep-IF (3.1 – 6 GHz) from the NWA to create the RF sweep from 15105 to 18005 MHz and a LO sweep from 15100 to 18000 MHz; RF is multiplied by 12 to generate 181.26 to 216.06 GHz. The difference frequency (RF – LO = 5 MHz) - multiplied by Nharmonic - generates the a1st and b1st first-IF of 60 MHz. The first-IF is mixed with 61.041667 MHz to create the a2nd and b2nd second-IF of 1.041667 MHz (the IF frequency of the NWA). A 10 MHz reference (not shown) is created by the second harmonic of the difference between the 12.005 and 12 GHz sources.

**FGPA-Based System**

To further understand the development of the FGPA-based system, an overview of SFCW signal processing and calibration must be explained. With our SFCW radar, complex baseband *I-Q* voltages of a set of *N* discrete frequencies separated by some  $\Delta f$  over a bandwidth *BW* are measured for both reference and received signals (*a* and *b*, respectively); that is, a sample of the transmitted signal *a* and the received signal *b* are recorded. This then

establishes  $\Gamma$ , a discrete and band-limited frequency-domain representation of the scene reflectivity.

$$\Gamma_k = \left. \frac{b_I + jb_Q}{a_I + ja_Q} \right|_k$$

Calibration is required to normalize the magnitude and phase of the *N* points measured. A flat, “optically-smooth” reflector plate is placed at some known distance; in practice, the calibration plate is generally at a range



Figure 3 • FPGA – based receiver and sweep- source. (1) 60 MHz, 8 MHz BW filters. (2) 30 dB IF amplifiers. (3) Hittite HMCAD 1520 evaluation board. (4) Xilinx SP601 FPGA evaluation board. (5) Linear Technologies 6946-3 PLL/VCO evaluation board. (6) Reference digitizer.

similar to the features that are to be measured. The calibration coefficients  $\Gamma_{reference}$  are stored prior to use and calibrated data  $\Gamma_{calibrated}$  is computed from the ratio of the measured and reference values; this is analogous to the thru calibration of a vector network analyzer.

$$\Gamma_{calibrated} = \frac{\Gamma_{measured}}{\Gamma_{reference}}$$

Visual inspection of the data would require viewing in the time-domain. An inverse-transform, such as the Inverse Discrete Fourier Transform (IDFT), can be computed and the alias-free time  $T_{AF}$  is limited to the number of points  $N$  measured and the radar bandwidth  $BW$ . The spatial domain is given by multiplying time by  $v/2$  (the round-trip speed of light).

$$T_{AF} = \frac{N - 1}{BW}$$

It is often the case that one wishes to see a “zoomed” view in the time domain, a common option in NWAs. We use a chirp transform algorithm, loosely referred to by us as the “Inverse” Chirp Z-Transform (ICZT), to zoom in on time-domain features of interest. Similar to the analysis and synthesis Discrete Fourier Transform (DFT, IDFT) equations, a synthesis equation for the ICZT can be inferred from the chirp Z-transform.

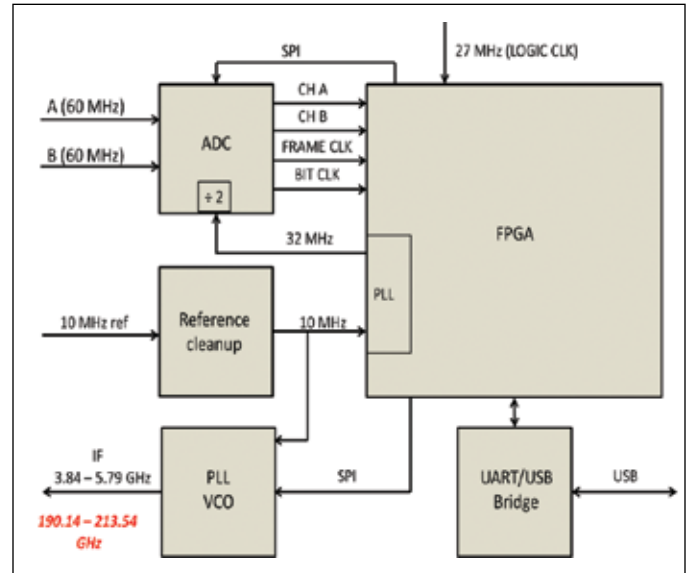


Figure 4 • FPGA- based system overview. The 10 MHz reference is digitized and passed to the PLL+VCO to create the sweep-IF and a FPGA resource PLL for the sample clock. Data is pipelined through mixing and integration stages and sent along to a PC via USB.

$$A = e^{\frac{j2\pi T_{start}}{T_{AF}}}$$

$$W = e^{\frac{-j2\pi (T_{end}-T_{start})}{N T_{AF}}}$$

$$x[n] = \frac{1}{N} \sum_{k=0}^{N-1} \Gamma'[k] A^k W^{-kn}$$

$$t[n] = \frac{n (T_{end} - T_{start})}{N - 1} + T_{start}$$

$A$  and  $W$  are complex arguments that define the starting and indexing values of points in the Z plane; we compute a special case of the transform along the unit circle, thereby fixing  $|A| = |W| = 1$ . We can define  $A$  and  $W$  as functions of the alias-free time  $T_{AF}$ , desired viewing start time  $T_{start}$  and desired end time  $T_{end}$ . Also, frequency-domain information  $\Gamma$  is windowed with a Kaiser function  $\beta$  such that  $\Gamma'_k = \Gamma_k \cdot \beta_k$ . The time-domain information  $x$  is now presented for an arbitrary time  $t$ . Similar to the DFT equations, computation is typically done using the Fast-Fourier Transform (FFT).

The real-time signal processing on the FPGA is akin to a software defined radio designed for use with a single-carrier; the data is sampled and mixed with a fixed digi-

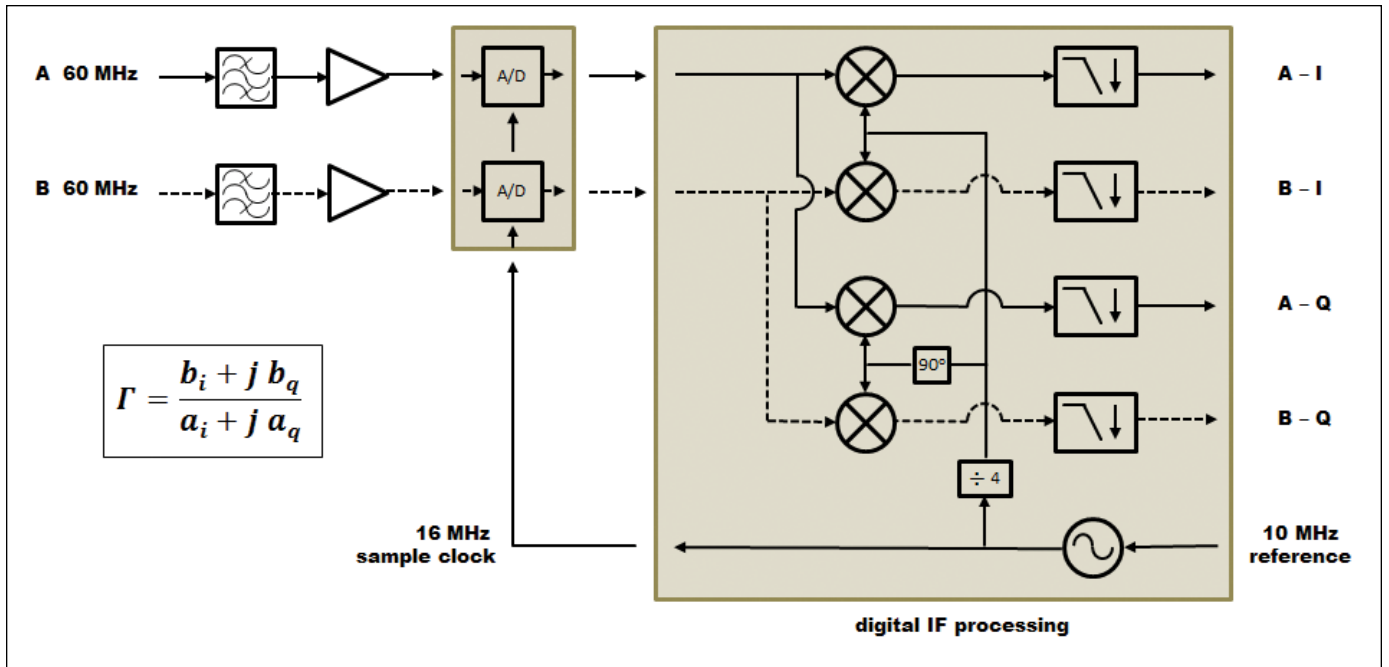


Figure 5 • Concept overview for sampling, base-banding, and filtering of the IF signals. The mixers are implemented as a four-state state machine multiplying time samples by {1, 0, -1, 0} for in-phase and {0, -1, 0, 1} for quadrature channels.

tal-LO to baseband. Usually, the digital-local-oscillator (LO) for a single-carrier system is implemented as a complex look-up table where the real component is mixed with the signal for in-phase *I* and the imaginary part is used for quadrature *Q*. In our system, the LO and mixer are further simplified by careful selection of sampling frequency,  $f_s = 16 \text{ Msps}$ . Under-sampling the 60 MHz IF at 16 Msps aliases the digital IF signal to 4 MHz, equal to  $f_s/4$ . A well-known base-banding technique is to multiply the  $f_s/4$  signal with sequence of ones, zeros, and negative ones. Evaluating a LO of  $f_s/4$  yields an in-phase multiplication sequence of {1, 0, -1, 0} and a quadrature sequence {0, -1, 0, 1} for even-numbered Nyquist zones (we sample in the 8th) (Figure 5). The mixer is simply a state-machine multiplying the sampled time-series by ones, zeros, or negative ones; other LO time series would introduce spectral spurs in addition to growing of the data register-size prior to filtering.

The baseband signals require filtering as well as integration to ameliorate the high noise levels inherent in MMW systems. Our approach is to combine decimation, filtering, and integration stages using Cascaded Integrator-Comb (CIC) filters. A stationary SFCW radar measures *I* and *Q* at 0 Hz and the typical roll-off concerns of decimating CIC filters as applied to software-defined radio are used to our advantage; no other digital filtering or integration is required after the CIC filter stage. Filtering and integration implies register growth and processed data is truncated to a convenient 32 bit resolu-

tion (for each I and Q component of *a* and *b*, i.e. 128 bits per frequency step). It was estimated that we would require a processing gain around 40 dB to adequately measure the scene with the MMW radar; setting parameters of the CIC filters such that the group delay is equal to 8096 samples, a convenient power of 2, provides a filter bandwidth of approximately 1 kHz and a processing gain  $G_p$  of 39 dB.

$$G_p = -10 \log_{10} (1 \text{ kHz} / 8 \text{ MHz}) \approx 10 \log_{10} (8096) \approx 39 \text{ dB}$$

To compare the NWA- and FPGA-based systems, a test setup was devised such that both systems could multiplex the OML modules; to properly evaluate both systems and facilitate calibration, the IF channels *a* and *b* were split to the NWA and the FPGA-based receiver (indicating a 3 dB loss in sensitivity, but acceptable for our demonstration) and the microwave sweep-source was electromagnetically switched. The Linear 6946-3 was configured so that  $\Delta f = f_{\text{reference}} = 10 \text{ MHz}$  and was swept 3.84 – 5.79 GHz yielding 196 points to measure. The NWA could measure 201 points. In the effort that both systems measured identical frequency points, the NWA was swept 3.84 – 5.84 GHz and the last 5 data points were discarded.

Once the test setup was arranged, the calibration plate was placed down-range. For the NWA-based system, calibration consists of thru-normalization of the *b/a* channel. In the FPGA-based system, the frequency domain data  $\Gamma_{\text{calibrated}}$  are recorded. The systems were then allowed to run for five minutes and then calibrated data for both

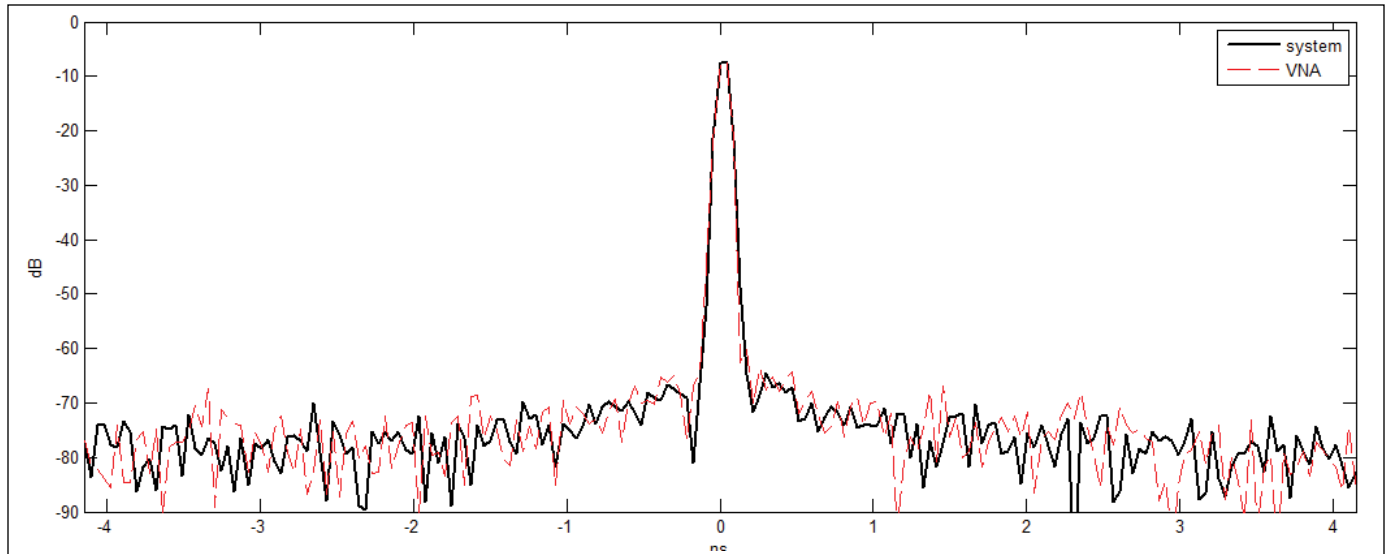


Figure 6 • NWA- and FPGA-based systems viewing plate 5 minutes after calibration. Clearly, both systems have similar SNR and phase-stability.

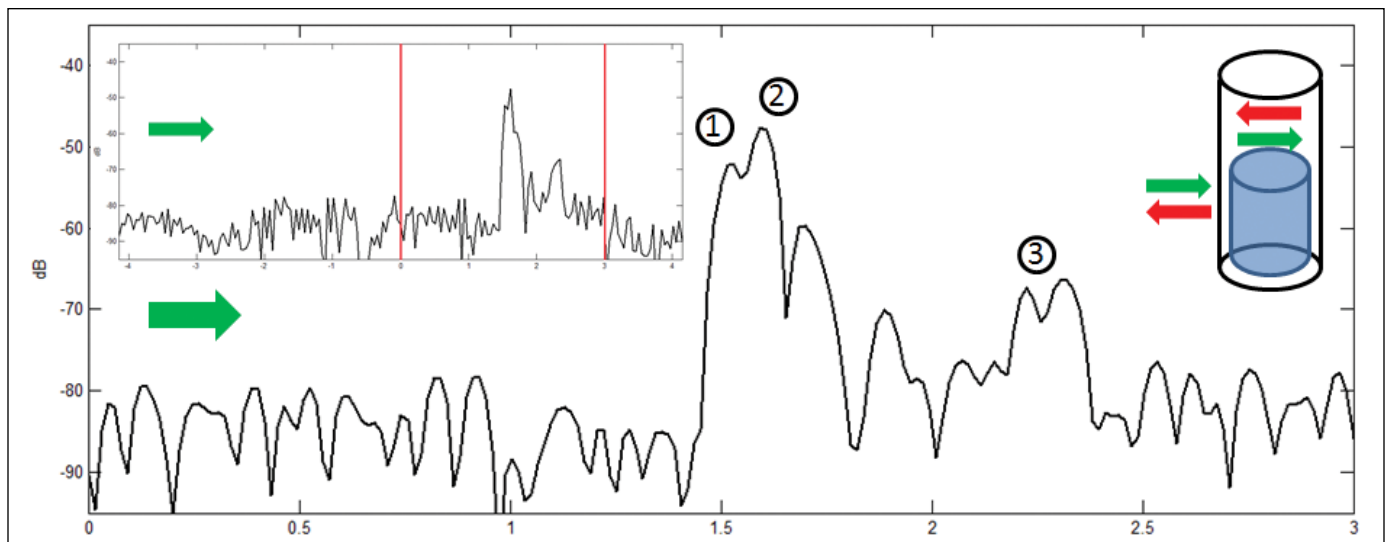


Figure 7 • FPGA-based system measuring thickness and dimensions of ABS plastic pipe sleaving shorter steel pipe. Data is shown in the time-domain using ICZT. Relief in upper-left corner shows the full time-transform while upper-right shows pipe arrangement. The radar “views” the scene from the left side and sees the reflection of the ABS pipe (1) followed by a reflection from the steel tube (2) and later sees the rear of the ABS tube (3) as it is positioned such that it will glance over the steel tube.

was recorded. Figure 6 demonstrates that data viewed in the time-domain shows very strong agreement of SNR and phase-stability for a similar sweep time of approximately 250 ms (i.e. integration time). While the FPGA-based MMW radar has not been tested in a boiler setting, a quick demonstration of its ability is shown when viewing a steel tube with an ABS plastic tube coating (Figure 7) where plastic thickness and tube diameter are easily calculated from the time-domain.

In summary, we have successfully constructed a FPGA-based replacement of the NWA for our instrumentation-based radar. Several important factors were adhered to

during design and demonstrated here. First, it was required that we maintain 70 dB SNR at calibration for adequate imaging of the boiler. Second, long-term phase-stability must be maintained for a system that will not see calibration as often as would be done in the laboratory. Third, a maximum sweep-time of 250 ms was observed; the boiler environment is one that experiences low-frequency vibrations and imaging resolution would be reduced should sweep-time increase. Furthermore, a means to view MMW data over varying time-scales is presented using our so-named ICZT. Finally, we show that an aggressive under-sampling scheme can be used to sample with higher-prec-

sion as well as reduce complexity of FPGA design and timing-constraints. While a NWA is an extremely valuable and requisite tool in the laboratory, the FPGA-based system presents itself as a suitable replacement for dedicated MMW service at a much-lower cost. Future work will include a more versatile frequency synthesizer such that the system may be used in different scenarios and with different bands. Additionally, an ARM-based computer will be added to facilitate network connections, control the radar positioner, and to compute test parameters locally.

#### About the Authors:

John Mower, originally a farmer with brief career stints in the logging and excavating industries, received his BSEE and MSEE degrees from the University of Washington, (2010 and 2012), where he studied electromagnetics and millimeter-wave remote sensing. He is currently a research engineer in the Air-Sea Interaction and Remote-Sensing department of the Applied Physics Laboratory – University of Washington. His current work entails a multi-antenna X-band marine wave-sensing radar. Always happy to discuss radar, radio, and remote sensing, he can be reached at mowerj@apl.washington.edu or john.m.mower@gmail.com.

Dr. Kuga is a Professor of Electrical Engineering at the University of Washington. He received his B.S., M.S., and Ph.D. degrees from the University of Washington, Seattle

in 1977, 1979, and 1983, respectively. From 1983 to 1988, he was a Research Assistant Professor of Electrical Engineering at the University of Washington. From 1988 to 1991, he was an Assistant Professor of Electrical Engineering and Computer Science at The University of Michigan. Since 1991, he is with the University of Washington. He was an Associate Editor of *Radio Science* (1993-1996) and *IEEE Trans. Geoscience and Remote Sensing* (1996-2000). He was elected to IEEE Fellow in 2004. His research interests are in the areas of microwave and millimeter-wave remote sensing, high frequency devices and materials, and optics. kuga@ee.washington.edu

#### References:

J. Mower, Y. Kuga, P. Ariessohn, and G. Kychakoff, "A Millimeter-wave Imaging System for Kraft Recovery Boilers," *IEEE APS/URSI*, Spokane, WA. July 2011.

K. B. Cooper, R. J. Dengler, G. Chattopadhyay, E. Schlecht, J. Gill, A. Skalare, I. Mehdi, P. H. Siegel, "A high-resolution imaging radar at 580 GHz," *IEEE Microwave and Wireless Components Letters*, vol.18, no. 1, pp. 64-66, Jan. 2008.

E.B. Hogenauer, "An economical class of digital filters for decimation and interpolation", *IEEE Transactions on Accoustics, Speech, and Signal Processing*, vol. ASSP-29, pp.155-162, April 1981.

L. Rabiner, R. Schafer, and C. Rader. "The chirp z-transform algorithm." *IEEE Transactions on Audio and Electroacoustics*, vol. au-17, 2, pp. 86-92, June 1969.